

Expectation Propagation Line Spectral Estimation

Jiang Zhu and Mihai-Alin Badiu

Abstract

Line spectral estimation (LSE) is a fundamental problem in signal processing fields, as it arises in various fields such as radar signal processing and communication fields. This paper develops expectation propagation (EP) based LSE (EPLSE) method. The proposed method automatically estimates the model order, noise variance, and can deal with the nonlinear measurements. Numerical experiments show the excellent performance of EPLSE.

Keywords: Expectation propagation, line spectral estimation, model order estimation, nonlinear measurements

I. INTRODUCTION

Line spectral estimation [1] aiming to extract the frequencies of a mixture of sinusoids is a fundamental problem in signal processing fields, as it arises in numerous disciplines in engineering, physics, and natural sciences such as radar signal processing, channel estimation, etc [2, 3]. Classical methods including maximum likelihood (ML) [4] or subspace methods such as MUSIC and ESPRIT [5–7]. The ML approach involves maximizing a nonconvex function which has a multimodal shape with a sharp global maximum, which requires accurate initialization. Compared to subspace based approaches, ML performs better when the measurements or the SNR is small.

Compressed sensing (CS) based approaches which exploit the sparsity of the frequency domain are proposed. By discretizing the frequency into a number of grids to construct a dictionary matrix, the original nonlinear frequency estimation problem is transformed to be a sparse linear inverse problem [8]. Since the frequency is continuous-valued, discretization incurs grid mismatch [9]. As a result, off-grid methods are proposed, which refine the grid gradually to overcome the grid mismatch effectively [10–14].

J. Zhu is with Ocean College, Zhejiang University, Zhoushan 316021, China (e-mail: jiangzhu16@zju.edu.cn). M. Badiu is with the Department of Engineering Science, University of Oxford, Parks Road, Oxford, OX1 3PJ, UK, (email: mi-hai.badiu@eng.ox.ac.uk).

To work directly with continuously parameterized dictionaries, gridless methods are proposed and can be classified into two categories: atomic norm based [15–22] and variational LSE (VALSE) [23, 24] approaches. The atomic norm based approaches allow for working with an infinite, continuous dictionary and are proved to recover the well separated frequencies perfectly in the noiseless case. While for the VALSE, it treats the frequency as random variables, and it automatically estimates the model order, the noise variance and the posterior probability density functions (PDF) of the frequencies. As for the computation complexity, the atomic norm based approaches involve solving a semidefinite programming (SDP), which is usually very high. In contrast, VALSE can be implemented with much lower computation complexity.

From the Bayesian algorithm point of view, approximate message passing (AMP) [25] and generalized approximate message passing (GAMP) [26] are proposed to deal with the sparse signal recovery from linear and nonlinear measurements. It is shown that both AMP and GAMP can be derived from expectation propagation (EP) [27–32]. By treating the frequency and amplitudes as random variables and formalize the factor graph, we derive EP LSE (EPLSE). We adopt the Bernoulli Gaussian prior distribution to estimate the model order. In addition, expectation maximization (EM) is incorporated to iteratively learn both the parameters of the prior and output distribution [33].

For a univariate function $f(\cdot) : \mathbb{R} \rightarrow \mathbb{R}$, let $\dot{f}(\cdot)$ and $\ddot{f}(\cdot)$ denote the first and second derivative of $f(\cdot)$, respectively. $\mathcal{CN}(\mathbf{x}; \boldsymbol{\mu}, \boldsymbol{\Sigma})$ denote the complex normal distribution of \mathbf{x} with mean $\boldsymbol{\mu}$ and covariance $\boldsymbol{\Sigma}$, and let $\mathcal{VM}(\theta, \mu, \kappa)$ denote the von Mises distribution of θ with mean direction μ and concentration parameter κ . Let $\Re\{\cdot\}$ return the real part. Let \mathbf{I}_L denote the identity matrix of dimension L . For a distribution $p(\mathbf{x})$, let $\text{Proj}[p(\mathbf{x})] \triangleq \mathcal{CN}(\mathbf{x}; \boldsymbol{\mu}, \text{diag}(\boldsymbol{\sigma}^2))$ with mean $\boldsymbol{\mu} = \mathbb{E}_{\mathbf{x} \sim p(\mathbf{x})}[\mathbf{x}]$ and variances $\boldsymbol{\sigma}^2 = \text{Var}_{\mathbf{x} \sim p(\mathbf{x})}[\mathbf{x}]$. For a set \mathcal{M} , let $|\mathcal{M}|$ denotes its cardinality. For a complex vector $\mathbf{x} \in \mathbb{C}^n$, $|\mathbf{x}|$ returns its elementwise magnitude.

II. PROBLEM SETUP

Let $\mathbf{z} \in \mathbb{C}^M$ be a line spectrum signal consisting of K complex sinusoids

$$\mathbf{z} = \sum_{k=1}^K \mathbf{a}(\tilde{\theta}_k) \tilde{x}_k, \quad (1)$$

where \tilde{x}_k is the complex amplitude of the k th frequency, $\tilde{\theta}_k \in [-\pi, \pi)$ is the k th frequency, and

$$\mathbf{a}(\theta) = [1, e^{j\theta}, \dots, e^{j(M-1)\theta}]^T. \quad (2)$$

The LSE undergoes a componentwise (linear or nonlinear) transform, which is described as a conditional PDF $p(\mathbf{y}|\mathbf{z}; \boldsymbol{\omega}_z)$

$$p(\mathbf{y}|\mathbf{z}; \boldsymbol{\omega}_z) = \prod_{m=1}^M p(y_m|z_m; \boldsymbol{\omega}_z), \quad (3)$$

where $\boldsymbol{\omega}_z$ are the unknown nuisance parameters. In the following text, we illustrate some examples about $p(\mathbf{y}|\mathbf{z})$.

- The LSE is corrupted by the additive white Gaussian noise and is described by

$$\mathbf{y} = \mathbf{z} + \mathbf{w}, \quad (4)$$

where $\mathbf{w} \sim \mathcal{CN}(\mathbf{w}; \mathbf{0}, \sigma^2 \mathbf{I}_M)$, σ^2 is the variance of the noise.

- Incomplete measurements, where only a subset $\mathcal{M} = \{m_1, \dots, m_M\} \subseteq \{0, 1, \dots, M-1\}$ of the measurements $\mathbf{y}_{\mathcal{M}}$ is observed.
- Quantized measurements [36]: $\mathbf{y} = Q(\mathbf{z} + \mathbf{w})$, where $Q(\cdot)$ denotes a quantizer which maps the continuous values into discrete numbers.
- Magnitude measurements [37]: $\mathbf{y} = |\mathbf{z} + \mathbf{w}|$, $\mathbf{y} = |\mathbf{z}| + \mathbf{w}$ or more generally $\mathbf{y} = |\mathbf{z} + \mathbf{w}| + \mathbf{v}$ where \mathbf{v} is also AWGN.
- Quantized magnitude measurements [38, 39]: $\mathbf{y} = Q(|\mathbf{z} + \mathbf{w}| + \mathbf{v})$, which is a concatenation of the magnitude and quantization nonlinear operations.
- Impulsive noise [40]: $\mathbf{y} = \mathbf{z} + \mathbf{w}$ and \mathbf{w} is non-Gaussian. For example, \mathbf{w} denotes the impulsive noise and follows a Laplace distribution.

For all the listed cases, $\boldsymbol{\omega}_z$ refers to the variance of the noise.

Since the sparsity level K is usually unknown, the line spectrum signal consisting of N complex sinusoids is assumed [23]

$$\mathbf{z} = \sum_{i=1}^N x_i \mathbf{a}(\theta_i) \triangleq \mathbf{A}(\boldsymbol{\theta}) \mathbf{x}, \quad (5)$$

where $\mathbf{A}(\boldsymbol{\theta}) = [\mathbf{a}(\theta_1), \dots, \mathbf{a}(\theta_N)]$ and $N \leq M$. For the frequencies and coefficients, i.i.d. Bernoulli Gaussian prior distribution is used, i.e.,

$$p(\boldsymbol{\theta}) = \prod_{n=1}^N p(\theta_n), \quad p(\mathbf{x}; \boldsymbol{\omega}_x) = \prod_{n=1}^N p(x_n; \boldsymbol{\omega}_x), \quad (6)$$

where

$$p(x_n; \boldsymbol{\omega}_x) = (1 - \pi_n) \delta(x_n) + \pi_n \mathcal{CN}(x_n; \mu_0, \tau_0), \quad (7)$$

$\boldsymbol{\omega}_x = [\pi_1, \dots, \pi_N, \mu_0, \tau_0]^T$ are unknown parameters. Note that Bernoulli Gaussian distribution can be imposed to enforce sparsity. For the prior distribution $p(\theta_n)$, von Mises distribution can be encoded [34]. For uninformative prior, we assume $p(\theta_n) = 1/(2\pi), \forall n$.

Let

$$\Theta = \{\boldsymbol{\theta}, \mathbf{x}, \mathbf{z}\}, \quad (8)$$

$$\boldsymbol{\omega} = \{\boldsymbol{\omega}_x, \boldsymbol{\omega}_z\} \quad (9)$$

be the set of all random variables and the model parameters, respectively. According to the Bayes rule, the joint PDF $p(\mathbf{y}, \Theta; \boldsymbol{\omega})$ is

$$p(\mathbf{y}, \Theta; \boldsymbol{\omega}) = p(\mathbf{y}|\mathbf{z})\delta(\mathbf{z} - \mathbf{A}(\boldsymbol{\theta})\mathbf{x}) \prod_{n=1}^N p(\theta_n)p(x_n; \boldsymbol{\omega}_x). \quad (10)$$

Given the above joint PDF (10), the type II maximum likelihood (ML) estimation of the model parameters $\hat{\boldsymbol{\omega}}_{\text{ML}}$ is

$$\hat{\boldsymbol{\omega}}_{\text{ML}} = \underset{\boldsymbol{\omega}}{\operatorname{argmax}} p(\mathbf{y}; \boldsymbol{\omega}) = \int p(\mathbf{y}, \Theta; \boldsymbol{\omega}) d\mathbf{z} d\Theta. \quad (11)$$

Then the minimum mean square error (MMSE) estimate of the parameters Θ is

$$\hat{\Theta} = \mathbb{E}[\Theta|\mathbf{y}; \boldsymbol{\omega}_{\text{ML}}], \quad (12)$$

where the expectation is taken with respect to

$$p(\Theta|\mathbf{y}; \hat{\boldsymbol{\omega}}_{\text{ML}}) = \frac{p(\mathbf{y}, \Theta; \hat{\boldsymbol{\omega}}_{\text{ML}})}{p(\mathbf{y}; \hat{\boldsymbol{\omega}}_{\text{ML}})} \quad (13)$$

Directly solving the ML estimate of $\boldsymbol{\omega}$ (11) or the MMSE estimate of Θ (12) are both intractable. As a result, an iterative algorithm is designed in Section III.

III. EPLSE ALGORITHM

The factor graph is presented in Fig. 1 and a delta factor node $\delta(\cdot)$ is introduced ¹. Before derivation, the following notations in Table I is used.

First, we initialize $m_{\delta \rightarrow z}(\mathbf{z}) = \mathcal{CN}(\mathbf{z}, \mathbf{z}_A^{\text{ext}}, \operatorname{diag}(\mathbf{v}_A^{\text{ext}}))$, $m_{n \rightarrow m}(x_n) \triangleq \mathcal{CN}(x_n; x_{n \rightarrow m}, \sigma_{n \rightarrow m}^2)$ and $m_{n \rightarrow m}(\theta_n) \triangleq \mathcal{VM}(\theta_n; \mu_{n \rightarrow m}, \kappa_{n \rightarrow m})$. Then we show how to update the messages to perform line spectral estimation.

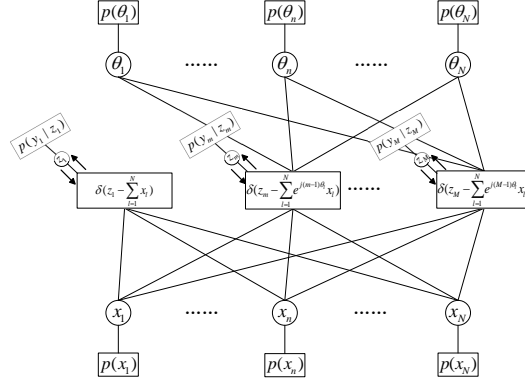


Fig. 1. The whole factor graph. Here we introduce a delta factor node $\delta(\cdot)$, which simplifies the calculation as shown later .

TABLE I
NOTATIONS USED FOR DERIVATION

$\tilde{m}_{\delta \rightarrow z_m}(z_m) \triangleq \mathcal{CN}(z_m; z_{A,m}^{\text{ext}}, v_{A,m}^{\text{ext}})$	The message from the factor node $\delta\left(z_m - \sum_{l=1}^N e^{j(m-1)\theta_l} x_l\right)$ to the variable node z_m
$m_{z_m \rightarrow \delta}(z_m) \triangleq \mathcal{CN}(z_m; z_{B,m}^{\text{ext}}, v_{B,m}^{\text{ext}})$	The message from the variable node z_m to the factor node $\delta\left(z_m - \sum_{l=1}^N e^{j(m-1)\theta_l} x_l\right)$
$\tilde{m}_{m \rightarrow n}(\theta_n) \triangleq \mathcal{VM}(\theta_n; \tilde{\mu}_{m \rightarrow n}, \tilde{\kappa}_{m \rightarrow n})$	The message from the factor node $\delta\left(z_m - \sum_{l=1}^N e^{j(m-1)\theta_l} x_l\right)$ to the variable node θ_n
$\tilde{m}_{m \rightarrow n}(x_n) \triangleq \mathcal{CN}(x_n; \tilde{\alpha}_{m \rightarrow n}, \tilde{\sigma}_{m \rightarrow n}^2)$	The message from the factor node $\delta\left(z_m - \sum_{l=1}^N e^{j(m-1)\theta_l} x_l\right)$ to the variable node x_n
$m_{n \rightarrow m}(\theta_n) \triangleq \mathcal{VM}(\theta_n; \mu_{n \rightarrow m}, \kappa_{n \rightarrow m})$	The message from the variable node θ_n to the factor node $\delta\left(z_m - \sum_{l=1}^N e^{j(m-1)\theta_l} x_l\right)$
$m_{n \rightarrow m}(x_n) \triangleq \mathcal{CN}(x_n; \alpha_{n \rightarrow m}, \sigma_{n \rightarrow m}^2)$	The message from the variable node x_n to the factor node $\delta\left(z_m - \sum_{l=1}^N e^{j(m-1)\theta_l} x_l\right)$

A. Update $m_{z \rightarrow \delta}(\mathbf{z})$

According to EP, $m_{\delta \rightarrow z}(\mathbf{z}) = \mathcal{CN}(\mathbf{z}, \mathbf{z}_A^{\text{ext}}(t), \text{diag}(\mathbf{v}_A^{\text{ext}}(t)))$ can be updated as

$$m_{z \rightarrow \delta}(\mathbf{z}) = \frac{\text{Proj} [m_{\delta \rightarrow z}(\mathbf{z}) p(\mathbf{y} | \mathbf{z}; \boldsymbol{\omega}_z^{\text{old}})]}{m_{\delta \rightarrow z}(\mathbf{z})} \triangleq \frac{\text{Proj} [q_B(\mathbf{z})]}{m_{\delta \rightarrow z}(\mathbf{z})}. \quad (14)$$

Then we calculate the componentwise posterior means and variances of \mathbf{z} with respect to $q_B(\mathbf{z})$ as

$$\mathbf{z}_B^{\text{post}} = \text{E} [\mathbf{z} | q_B(\mathbf{z})], \quad (15)$$

$$\mathbf{v}_B^{\text{post}} = \text{Var} [\mathbf{z} | q_B(\mathbf{z})]. \quad (16)$$

¹Such a factor graph was originally introduced in [30] for the generalized linear model (GLM), and a unified Bayesian inference framework for GLM was proposed.

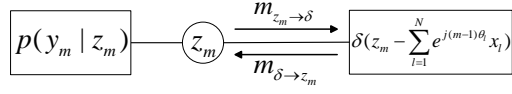


Fig. 2. The subfactor graph for updating $m_{z \rightarrow \delta}(\mathbf{z})$.

Therefore $\text{Proj}[q_B(\mathbf{z})]$ is ²

$$\text{Proj}[q_B(\mathbf{z})] = \mathcal{CN}(\mathbf{z}; \mathbf{z}_B^{\text{post}}, \text{diag}(\mathbf{v}_B^{\text{post}})). \quad (17)$$

According to (14), $m_{z \rightarrow \delta}(\mathbf{z})$ is calculated to be

$$m_{z \rightarrow \delta}(\mathbf{z}) = \mathcal{CN}(\mathbf{z}; \mathbf{z}_B^{\text{ext}}, \text{diag}(\mathbf{v}_B^{\text{ext}})), \quad (18)$$

where $\mathbf{v}_B^{\text{ext}}$ and $\mathbf{z}_B^{\text{ext}}$ are

$$\mathbf{v}_B^{\text{ext}}(t) = \left(\frac{1}{\mathbf{v}_B^{\text{post}}(t)} - \frac{1}{\mathbf{v}_A^{\text{ext}}(t)} \right)^{-1}, \quad (19a)$$

$$\mathbf{z}_B^{\text{ext}}(t) = \mathbf{v}_B^{\text{ext}}(t) \left(\frac{\mathbf{z}_B^{\text{post}}(t)}{\mathbf{v}_B^{\text{post}}(t)} - \frac{\mathbf{z}_A^{\text{ext}}(t)}{\mathbf{v}_A^{\text{ext}}(t)} \right). \quad (19b)$$

We also incorporate the expectation maximization (EM) algorithm to learn ω_z . The posterior distribution of \mathbf{z} is approximated as (17). We compute the expected complete log-likelihood function $\log p(\mathbf{y}|\mathbf{z}; \omega_z) + \log p(\mathbf{z})$ with respect to $p(\mathbf{z}|\mathbf{y}; \omega_z^{\text{old}})$, and drop the irrelevant terms to have

$$S(\omega_z; \omega_z^{\text{old}}) = \mathbb{E}_{q(\mathbf{z}|\mathbf{y}; \omega_z^{\text{old}})} [\log p(\mathbf{y}|\mathbf{z}; \omega_z)]. \quad (20)$$

Then ω_z is updated as

$$\omega_z^{\text{new}} = \underset{\omega_z}{\text{argmax}} S(\omega_z; \omega_z^{\text{old}}). \quad (21)$$

For the AWGN model

$$\mathbf{y} = \mathbf{z} + \mathbf{w}, \quad (22)$$

where $\mathbf{w} \sim \mathcal{CN}(\mathbf{w}; \mathbf{0}, \sigma_w^2 \mathbf{I})$, the posterior PDF $q(\mathbf{z}|\mathbf{y}; \omega_z^{\text{old}})$ is $q(\mathbf{z}|\mathbf{y}; \omega_z^{\text{old}}) = \text{Proj}[q_B(\mathbf{z})]$. Therefore we obtain

$$\sigma_w^2 = \frac{\|\mathbf{y} - \mathbf{z}_B^{\text{post}}\|^2 + \mathbf{1}^T \mathbf{v}_B^{\text{post}}}{M}. \quad (23)$$

²Note that for the linear measurement model $\mathbf{y} = \mathbf{z} + \mathbf{w}$, we have $\text{Proj}[q_B(\mathbf{z})] = q_B(\mathbf{z})$, i.e., the projection operation is unnecessary.

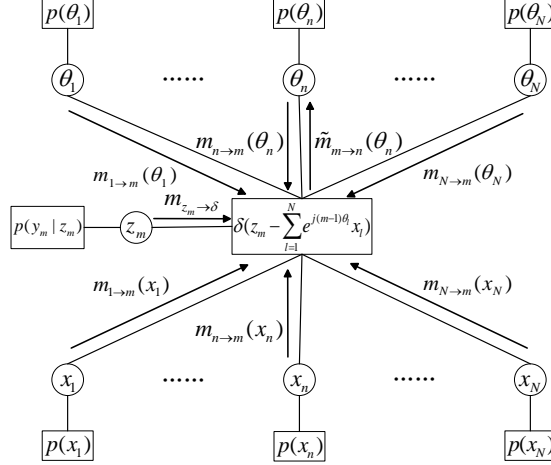


Fig. 3. The factor graph for calculating $\tilde{m}_{m \rightarrow n}(\theta_n)$.

For arbitrary $p(\mathbf{y}|\mathbf{z})$, we also obtain an approximate update equation. From the definition of $m_{z \rightarrow \delta}(\mathbf{z})$ and $\mathbf{z} = \mathbf{A}(\boldsymbol{\theta})\mathbf{x}$, we obtain an pseudo measurement model

$$\tilde{\mathbf{y}} = \mathbf{z} + \tilde{\mathbf{w}}, \quad (24)$$

where $\tilde{\mathbf{y}} = \mathbf{z}_{\text{B}}^{\text{ext}}$, $\tilde{\mathbf{w}} \sim \mathcal{CN}(\mathbf{w}; \mathbf{0}, \text{diag}(\tilde{\boldsymbol{\sigma}}^2))$ and $\tilde{\boldsymbol{\sigma}}^2 = \mathbf{v}_{\text{B}}^{\text{ext}}$. The noise variance σ_w^2 is updated as [41]

$$\sigma_w^2 = \frac{\|\tilde{\mathbf{y}} - \mathbf{z}_{\text{B}}^{\text{post}}\|^2 + \mathbf{1}^T \mathbf{v}_{\text{B}}^{\text{post}}}{M}. \quad (25)$$

Note that (25) includes (23) as a special case as for the AWGN case, $\tilde{\mathbf{y}} = \mathbf{y}$.

B. Updating of $\tilde{m}_{m \rightarrow n}(\theta_n)$

The subfactor graph is presented in Fig. 3. According to EP, $\tilde{m}_{m \rightarrow n}(\theta_n)$ is updated as

$$\begin{aligned} \tilde{m}_{m \rightarrow n}(\theta_n) &\propto \frac{\text{Proj} \left[\int \prod_{n=1}^N (m_{n \rightarrow m}(\theta_n) m_{n \rightarrow m}(x_n)) \delta \left(z_m - \left(\sum_{l=1}^N e^{j(m-1)\theta_l} x_l \right) \right) m_{z_m \rightarrow \delta}(z_m) \prod_{n=1}^N dx_n \prod_{l=1, l \neq n}^N d\theta_l dz_m \right]}{m_{n \rightarrow m}(\theta_n)} \\ &= \frac{\text{Proj} [e^{f_m(\theta_n)}]}{m_{n \rightarrow m}(\theta_n)}. \end{aligned} \quad (26)$$

Now we calculate the numerator term. First, $\delta \left(z_m - \left(\sum_{l=1}^N e^{j(m-1)\theta_l} x_l \right) \right)$ and $m_{z_m \rightarrow \delta}(z_m)$ implies the following pseudo measurement model

$$\begin{aligned} \tilde{y}_m &= e^{j(m-1)\theta_1} x_1 + \dots + e^{j(m-1)\theta_n} x_n + \dots + e^{j(m-1)\theta_N} x_N + \tilde{w} \\ &= e^{j(m-1)\theta_n} x_n + \underbrace{\left(\sum_{l=1, l \neq n}^N e^{j(m-1)\theta_l} x_l \right)}_{z_m} + \tilde{w}_m, \end{aligned} \quad (27)$$

where $\tilde{w}_m \sim \mathcal{CN}(\tilde{w}_m; 0, \tilde{\sigma}_m^2)$. Conditioned on θ_n , we approximate z_m as a Gaussian distribution by averaging over $\{\theta_l\}_{l \neq n}$ and $\{x_l\}_{l=1}^N$. Straightforward calculation yields

$$\begin{aligned} \mathbb{E}[z_m | \theta_n] &= e^{j(m-1)\theta_n} \mathbb{E}[x_n] + \sum_{l \neq n} \mathbb{E}\left[e^{j(m-1)\theta_l} x_l\right] \\ &= e^{j(m-1)\theta_n} x_{n \rightarrow m} + \underbrace{\sum_{l=1, l \neq n}^N e^{j(m-1)\mu_{l \rightarrow m}} \frac{I_{m-1}(\kappa_{l \rightarrow m})}{I_0(\kappa_{l \rightarrow m})} x_{l \rightarrow m}}_{v_{\setminus n, m_m}}, \end{aligned} \quad (28)$$

$$\begin{aligned} \text{Var}[z_m | \theta_n] &= \sigma_{n \rightarrow m}^2 + \sum_{l \neq n} \sigma_{l \rightarrow m}^2 + \sum_{l \neq n} |x_{l \rightarrow m}|^2 \left(1 - \left(\frac{I_{m-1}(\kappa_{l \rightarrow m})}{I_0(\kappa_{l \rightarrow m})}\right)^2\right) \\ &= \sum_{l=1}^N \sigma_{l \rightarrow m}^2 + \sum_{l \neq n} |x_{l \rightarrow m}|^2 \left(1 - \left(\frac{I_{m-1}(\kappa_{l \rightarrow m})}{I_0(\kappa_{l \rightarrow m})}\right)^2\right), \end{aligned} \quad (29)$$

which does not depend on θ_n and we use $\text{Var}[z_m]$ in the following text. Now we perform integration (26) with respect to z_m . Conditioned on θ_n , by viewing

$$z_m | \theta_n \sim \mathcal{CN}(z_m; \mathbb{E}[z_m | \theta_n], \text{Var}[z_m]), \quad (30)$$

and

$$\tilde{y}_m = z_m + \tilde{w}_m, \quad (31)$$

as the prior and likelihood of z_m , respectively, we perform integration over z_m to yield

$$\tilde{y}_m \sim \mathcal{CN}(\tilde{y}_m; e^{j(m-1)\theta_n} x_{n \rightarrow m} + v_{\setminus n, m_m}, \text{Var}[z_m] + \tilde{\sigma}_m^2). \quad (32)$$

Then $f_m(\theta_n)$ is

$$\begin{aligned} f_m(\theta_n) &= -\frac{|y_m - (e^{j(m-1)\theta_n} x_{n \rightarrow m} + v_{\setminus n, m_m})|^2}{\text{Var}[z_m] + \tilde{\sigma}_m^2} + \ln m_{n \rightarrow m}(\theta_n) + \text{const} \\ &= 2\Re\{y_{\setminus n, m}^r x_{n \rightarrow m}^* e^{-j(m-1)\theta_n}\} / (\tilde{\sigma}_m^2 + \text{Var}[z_m]) + \ln m_{n \rightarrow m}(\theta_n) \end{aligned} \quad (33)$$

$$= 2|y_{\setminus n, m}^r x_{n \rightarrow m}| \cos((m-1)\theta_n + \angle x_{n \rightarrow m} - \angle y_{\setminus n, m}^r) / (\tilde{\sigma}_m^2 + \text{Var}[z_m]) + \kappa_{n \rightarrow m} \cos(\theta_n - \mu_{n \rightarrow m}), \quad (34)$$

where

$$y_{\setminus n, m}^r = y_m - v_{\setminus n, m}. \quad (35)$$

Then we project $f_m(\theta_n)$ as a von Mises distribution

$$\text{Proj}\left[e^{f_m(\theta_n)}\right] = \mathcal{VM}(\theta_n; \mu_{m,n}, \kappa_{m,n}). \quad (36)$$

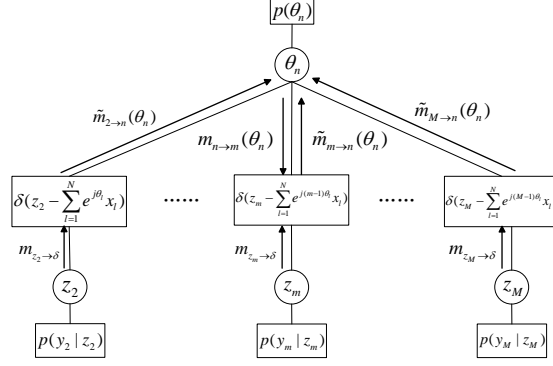


Fig. 4. The factor graph for calculating $m_{n \rightarrow m}(\theta_n)$.

Note that the PDF proportional to $e^{f_m(\theta_n)}$ is a product of wrapped normal distribution and von Mises distribution. Numerically, it was found that the maximum of $f_m(\theta_n)$ is near $\mu_{n \rightarrow m}$. Thus we perform a single Newton refinement at $\mu_{n \rightarrow m}$ and obtain the approximated von Mises distribution, as shown in VI-A.

As a result, using (26) we have

$$\tilde{\kappa}_{m \rightarrow n} e^{j\tilde{\mu}_{m \rightarrow n}} = \kappa_{m,n} e^{j\mu_{m,n}} - \kappa_{n \rightarrow m} e^{j\mu_{n \rightarrow m}}. \quad (37)$$

C. Updating of $m_{n \rightarrow m}(\theta_n)$

The subfactor graph is presented in Fig. 4.

$$\begin{aligned} m_{n \rightarrow m}(\theta_n) &\propto \frac{\text{Proj} \left[\prod_{m=1}^M \tilde{m}_{m \rightarrow n}(\theta_n) p(\theta_n) \right]}{\tilde{m}_{m \rightarrow n}(\theta_n)} \propto \frac{\text{Proj} \left[\prod_{m=1}^M \mathcal{VM}(\theta_n; \tilde{\mu}_{m \rightarrow n}, \tilde{\kappa}_{m \rightarrow n}) p(\theta_n) \right]}{\mathcal{VM}(\theta_n; \tilde{\mu}_{m \rightarrow n}, \tilde{\kappa}_{m \rightarrow n})} \\ &\triangleq \frac{\mathcal{VM}(\theta_n; \tilde{\mu}_n, \tilde{\kappa}_n)}{\mathcal{VM}(\theta_n; \tilde{\mu}_{m \rightarrow n}, \tilde{\kappa}_{m \rightarrow n})}, \end{aligned} \quad (38)$$

where

$$\kappa_{n \rightarrow m} e^{j\mu_{n \rightarrow m}} = \tilde{\kappa}_n e^{j\tilde{\mu}_n} - \tilde{\kappa}_{m \rightarrow n} e^{j\tilde{\mu}_{m \rightarrow n}}. \quad (39)$$

Given that we do not have any knowledge of prior distribution $p(\theta)$, $\kappa_{n \rightarrow m}$ and $\mu_{n \rightarrow m}$ is calculated to be

$$\kappa_{n \rightarrow m} e^{j\mu_{n \rightarrow m}} = \sum_{l=1, l \neq m}^M \tilde{\kappa}_{l \rightarrow n} e^{j\tilde{\mu}_{l \rightarrow n}}. \quad (40)$$

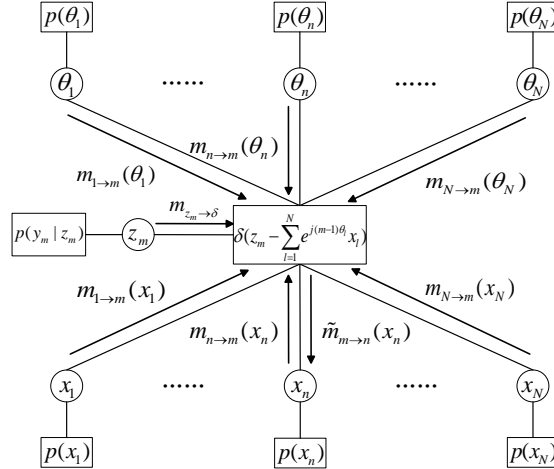


Fig. 5. The factor graph for calculating $\tilde{m}_{m \rightarrow n}(x_n)$.

D. Updating of $\tilde{m}_{m \rightarrow n}(x_n)$

The subfactor graph is presented in Fig. 5. $\tilde{m}_{m \rightarrow n}(x_n)$ can be updated as

$$\tilde{m}_{m \rightarrow n}(x_n) = \frac{\text{Proj} \left[\int \prod_{n=1}^N (m_{n \rightarrow m}(\theta_n) m_{n \rightarrow m}(x_n)) \delta \left(z_m - \left(\sum_{l=1}^N e^{j(m-1)\theta_l} x_l \right) \right) m_{z_m \rightarrow \delta}(z_m) \prod_{n=1}^N d\theta_n \prod_{l=1, l \neq n}^N dx_l \right]}{m_{n \rightarrow m}(x_n)} \quad (41)$$

$$= \frac{\text{Proj} [m_{n \rightarrow m}(x_n) e^{g_m(x_n)}]}{m_{n \rightarrow m}(x_n)}. \quad (42)$$

Similar to (27), $e^{g(x_n)}$ can be equivalently formulated as

$$\begin{aligned} & \int \left(\prod_{n=1}^N m_{n \rightarrow m}(\theta_n) \right) \left(\prod_{l=1, l \neq n}^N m_{l \rightarrow m}(x_l) \right) \delta \left(z_m - \left(\sum_{l=1}^N e^{j(m-1)\theta_l} x_l \right) \right) m_{z_m \rightarrow \delta}(z_m) \prod_{n=1}^N d\theta_n \prod_{l=1, l \neq n}^N dx_l \\ &= \int \left(\prod_{n=1}^N m_{n \rightarrow m}(\theta_n) \right) \left(\prod_{l=1, l \neq n}^N m_{l \rightarrow m}(x_l) \right) p(\tilde{y}_m | z_m) \\ & \quad \times \delta \left(z_m - e^{j(m-1)\theta_n} x_n - \left(\sum_{l \neq n} e^{j(m-1)\theta_l} x_l \right) \right) \prod_{n=1}^N d\theta_n \prod_{l=1, l \neq n}^N dx_l dz_m. \end{aligned} \quad (43)$$

Conditioned on x_n , we approximate z_m as a Gaussian distribution by averaging over $\{x_l\}_{l \neq n}$ and $\{\theta_l\}_{l=1}^N$. Straightforward calculation yields

$$\mathbb{E}[z_m|x_n] = \mathbb{E}\left[e^{j(m-1)\theta_n}\right] x_n + \sum_{l \neq n} \mathbb{E}\left[e^{j(m-1)\theta_l} x_l\right] \quad (44)$$

$$= e^{j(m-1)\mu_{n \rightarrow m}} \frac{I_{m-1}(\kappa_{n \rightarrow m})}{I_0(\kappa_{n \rightarrow m})} x_n + \underbrace{\sum_{l \neq n} e^{j(m-1)\mu_{l \rightarrow m}} \frac{I_{m-1}(\kappa_{l \rightarrow m})}{I_0(\kappa_{l \rightarrow m})} x_{l \rightarrow m}}_{v_{\setminus n, m}} \quad (45)$$

$$= \lambda_{n \rightarrow m} x_n + v_{\setminus n, m}, \quad (46)$$

$$\begin{aligned} \text{Var}[z_m|x_n] &= |x_n|^2 \left(1 - \left(\frac{I_{m-1}(\kappa_{n \rightarrow m})}{I_0(\kappa_{n \rightarrow m})}\right)^2\right) + \sum_{l \neq n} \sigma_{l \rightarrow m}^2 + \sum_{l \neq n} |x_{l \rightarrow m}|^2 \left(1 - \left(\frac{I_{m-1}(\kappa_{l \rightarrow m})}{I_0(\kappa_{l \rightarrow m})}\right)^2\right) \\ &= \delta_{n \rightarrow m}^2 |x_n|^2 + \nu_{\setminus n, m}, \end{aligned} \quad (47)$$

Thus

$$\begin{aligned} g_m(x_n) &= (\approx) - \frac{|\tilde{y}_m - v_{\setminus n, m} - \lambda_{n \rightarrow m} x_n|^2}{\text{Var}[z_m|x_n] + \tilde{\sigma}_m^2} - \ln(\text{Var}[z_m|x_n] + \tilde{\sigma}_m^2) + \text{const} \\ &= - \frac{|\tilde{y}_m - v_{\setminus n, m} - \lambda_{n \rightarrow m} x_n|^2}{\delta_{n \rightarrow m}^2 |x_n|^2 + \nu_{\setminus n, m} + \tilde{\sigma}_m^2} - \ln(\delta_{n \rightarrow m}^2 |x_n|^2 + \nu_{\setminus n, m} + \tilde{\sigma}_m^2) + \text{const}. \end{aligned} \quad (48)$$

Then we project $m_{n \rightarrow m}(x_n) e^{g_m(x_n)}$ as a Gaussian distribution. For simplicity, we first project $e^{g_m(x_n)}$ as a Gaussian distribution. Then we have

$$\tilde{m}_{m \rightarrow n}(x_n) = \mathcal{CN}(x_n; \tilde{x}_{m \rightarrow n}, \tilde{\sigma}_{m \rightarrow n}^2) = \text{Proj}\left[e^{g_m(x_n)}\right]. \quad (49)$$

According to (48), we approximate $\tilde{x}_{m \rightarrow n}$ and $\tilde{\sigma}_{m \rightarrow n}^2$ as

$$\tilde{x}_{m \rightarrow n} = \frac{\tilde{y}_m - v_{\setminus n, m}}{\lambda_{n \rightarrow m}}, \quad (50a)$$

$$\tilde{\sigma}_{m \rightarrow n}^2 = \frac{\delta_{n \rightarrow m}^2 |x_n|^2 + \nu_{\setminus n, m} + \tilde{\sigma}_m^2}{|\lambda_{n \rightarrow m}|^2} \Big|_{x_n = \tilde{x}_{m \rightarrow n}} = \frac{\delta_{n \rightarrow m}^2 |\tilde{x}_{m \rightarrow n}|^2 + \nu_{\setminus n, m} + \tilde{\sigma}_m^2}{|\lambda_{n \rightarrow m}|^2}. \quad (50b)$$

E. Updating of $m_{n \rightarrow m}(x_n)$

The subfactor graph is presented in Fig. 6. According to EP, $m_{n \rightarrow m}(x_n)$ is updated as

$$m_{n \rightarrow m}(x_n) \triangleq \mathcal{CN}(x_n; x_{n \rightarrow m}, \sigma_{n \rightarrow m}^2) \propto \frac{\text{Proj}\left[\prod_{m=1}^M \tilde{m}_{m \rightarrow n}(x_n) p(x_n)\right]}{\tilde{m}_{m \rightarrow n}(x_n)} \triangleq \frac{\text{Proj}\left[\mathcal{CN}(x_n; r_n, \sigma_n^2) p(x_n)\right]}{\mathcal{CN}(x_n; \tilde{x}_{m \rightarrow n}, \tilde{\sigma}_{m \rightarrow n}^2)}, \quad (51)$$

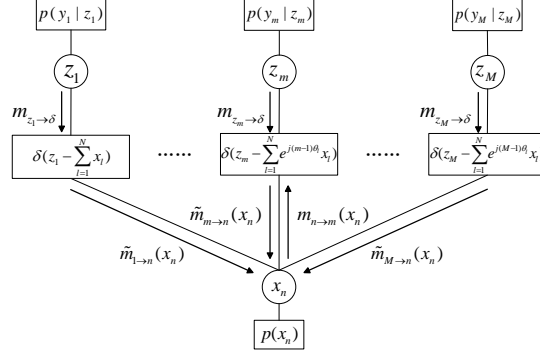


Fig. 6. The factor graph for calculating $m_{n \rightarrow m}(x_n)$.

where

$$\frac{1}{\sigma_n^2} = \sum_{m=1}^M \frac{1}{\tilde{\sigma}_{m \rightarrow n}^2}, \quad (52)$$

$$\frac{r_n}{\sigma_n^2} = \sum_{m=1}^M \frac{\tilde{x}_{m \rightarrow n}}{\tilde{\sigma}_{m \rightarrow n}^2}. \quad (53)$$

Let

$$\text{Proj} [\mathcal{CN}(x_n; r_n, \sigma_n^2) p(x_n; \boldsymbol{\omega})] = \mathcal{CN}(x_n; \hat{m}_n, \hat{v}_n^2), \quad (54)$$

then

$$\frac{1}{\sigma_{n \rightarrow m}^2} = \frac{1}{\hat{v}_n^2} - \frac{1}{\tilde{\sigma}_{m \rightarrow n}^2}, \quad (55)$$

$$\frac{x_{n \rightarrow m}}{\sigma_{n \rightarrow m}^2} = \frac{\hat{m}_n}{\hat{v}_n^2} - \frac{\tilde{x}_{m \rightarrow n}}{\tilde{\sigma}_{m \rightarrow n}^2}. \quad (56)$$

For (54), when the prior parameters $\boldsymbol{\omega}_x$ are unknown, we use the expectation maximization (EM) to learn these parameters. Let $\boldsymbol{\omega}_x^{\text{old}}$ denote the previous learned parameters. By viewing $x_n \sim p(x_n; \boldsymbol{\omega}_x^{\text{old}}) = (1 - \pi_n^{\text{old}})\delta(x_n) + \pi_n^{\text{old}}\mathcal{CN}(x_n; \mu_0^{\text{old}}, \tau_0^{\text{old}})$ as the prior distribution, and the pseudo decoupled measurement model

$$r_n = x_n + \tilde{v}_n \quad (57)$$

with conditional PDF $p(r_n|x_n) = \mathcal{CN}(x_n; r_n, \sigma_n^2)$. Then the posterior distribution of x_n is

$$p(x_n|y_n; \boldsymbol{\omega}_x^{\text{old}}) = (1 - \lambda_n^{\text{old}})\delta(x_n) + \lambda_n^{\text{old}}\mathcal{CN}(x_n; m_n^{\text{old}}, V_n^{\text{old}}),$$

where

$$m_n^{\text{old}} = \frac{\tau_0^{\text{old}}r_n + \sigma_n^2\mu_0^{\text{old}}}{\sigma_n^2 + \tau_0^{\text{old}}}, \quad V_n^{\text{old}} = \frac{\tau_0^{\text{old}}\sigma_n^2}{\sigma_n^2 + \tau_0^{\text{old}}}, \quad (58)$$

$$\lambda_n^{\text{old}} = \frac{\pi_n^{\text{old}}}{\pi_n^{\text{old}} + (1 - \pi_n^{\text{old}}) \exp(-M_n^{\text{old}})}, \quad (59)$$

where M_n^{old} in (59) is

$$M_n^{\text{old}} = \ln \frac{\sigma_n^2}{\sigma_n^2 + \tau_0^{\text{old}}} + \frac{|r_n|^2}{\sigma_n^2} - \frac{|r_n - \mu_0^{\text{old}}|^2}{\sigma_n^2 + \tau_0^{\text{old}}}. \quad (60)$$

Consequently, the posterior mean and variance are

$$\hat{m}_n = \lambda_n^{\text{old}} m_n^{\text{old}}, \quad (61a)$$

$$\hat{v}_n^2 = \lambda_n^{\text{old}} (|m_n^{\text{old}}|^2 + V_n^{\text{old}}) - |\lambda_n^{\text{old}} m_n^{\text{old}}|^2. \quad (61b)$$

Then we use the EM algorithm to update ω_x . We calculate the expected complete log-likelihood function with respect to $p(x_n|y_n; \omega_x^{\text{old}})$. After dropping the irrelevant terms, we obtain

$$Q(\omega_x, \omega_x^{\text{old}}) = \sum_{n=1}^N \left((1 - \lambda_n^{\text{old}}) \ln(1 - \pi_n) + \lambda_n^{\text{old}} \ln \pi_n - \lambda_n^{\text{old}} \left(\frac{|m_n^{\text{old}} - \mu_0|^2 + V_n^{\text{old}}}{\tau_0} + \ln(\pi \tau_0) \right) \right). \quad (62)$$

By setting $\partial Q(\omega_x, \omega_x^{\text{old}})/\partial \omega_x = \mathbf{0}$, one obtains

$$\pi_n^{\text{new}} = \lambda_n^{\text{old}}, \quad (63a)$$

$$\mu_0^{\text{new}} = \sum_{n=1}^N \lambda_n^{\text{old}} m_n^{\text{old}} / \sum_{n=1}^N \lambda_n^{\text{old}}, \quad (63b)$$

$$\tau_0^{\text{new}} = \sum_{n=1}^N \lambda_n^{\text{old}} [(\mu_0^{\text{old}} - m_n^{\text{old}})^2 + V_n^{\text{old}}] / \sum_{n=1}^N \lambda_n^{\text{old}}. \quad (63c)$$

F. Update of $m_{\delta \rightarrow z_m}(z_m)$

The message $m_{\delta \rightarrow z_m}(z_m)$ can be calculated as

$$\begin{aligned} m_{\delta \rightarrow z_m}(z_m) &= \frac{\text{Proj} \left[\int \prod_{n=1}^N (m_{n \rightarrow m}(\theta_n) m_{n \rightarrow m}(x_n)) \delta \left(z_m - \left(\sum_{l=1}^N e^{j m_m \theta_l} x_l \right) \right) m_{z_m \rightarrow \delta}(z_m) \prod_{n=1}^N dx_n \prod_{l=1}^N d\theta_l \right]}{m_{z_m \rightarrow \delta}(z_m)} \\ &= \frac{\text{Proj} [q_A(z_m) m_{z_m \rightarrow \delta}(z_m)]}{m_{z_m \rightarrow \delta}(z_m)}. \end{aligned} \quad (64)$$

We first approximate $q_A(z_m)$ as a Gaussian distribution, then we have

$$m_{\delta \rightarrow z_m}(z_m) = \text{Proj} [q_A(z_m)]. \quad (65)$$

The means and variances of z_m with respect to $q_A(z_m)$ can be easily calculated, which is

$$z_{A,m}^{\text{ext}}(t) = \sum_{l=1}^N \mathbb{E} \left[e^{j(m-1)\theta_l} x_l \right] = \sum_{l=1}^N e^{j(m-1)\mu_{l \rightarrow m}} \frac{I_{m-1}(\kappa_{l \rightarrow m})}{I_0(\kappa_{l \rightarrow m})} x_{l \rightarrow m}, \quad (66)$$

$$v_{A,m}^{\text{ext}}(t) = \sum_{l=1}^N \sigma_{l \rightarrow m}^2 + \sum_{l=1}^N |x_{l \rightarrow m}|^2 \left(1 - \left(\frac{I_{m-1}(\kappa_{l \rightarrow m})}{I_0(\kappa_{l \rightarrow m})} \right)^2 \right), \quad (67)$$

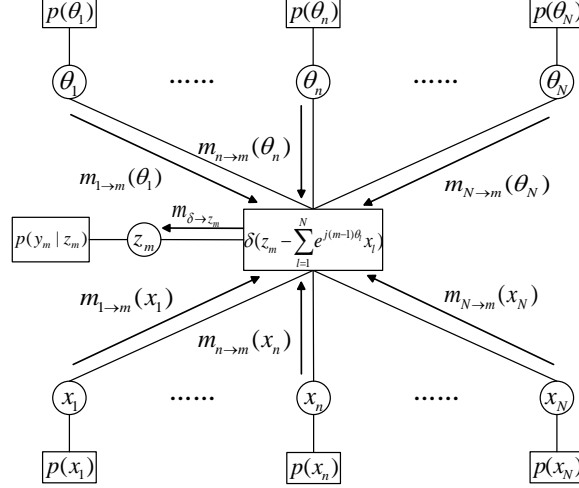


Fig. 7. The factor graph for calculating $m_{\delta \rightarrow z_m}(z_m)$.

Using (65) we obtain $m_{\delta \rightarrow z_m}(z_m)$ as

$$m_{\delta \rightarrow z_m}(z_m) = \mathcal{CN}(z_m; \mathbf{z}_{A,m}^{\text{ext}}, v_{A,m}^{\text{ext}}). \quad (68)$$

Note that the message $m_{\delta \rightarrow z_m}(z_m)$ is used to obtain $m_{z_m \rightarrow \delta}(z_m)$. For the linear measurement model $y_m = z_m + w_m$ with known variance σ_w^2 , $m_{z_m \rightarrow \delta}(z_m)$ is just $m_{z_m \rightarrow \delta}(z_m) = \mathcal{CN}(z_m; y_m, \sigma_w^2)$,

Now we close the loop of the algorithm. For EPLSE, the initialization provided by the VALSE [23] is adopted. Suppose that VALSE initialize $\mathbf{x} \in \mathbb{C}^N$ with the estimate and covariance matrix as $\hat{\mathbf{x}}_V$ and $\hat{\mathbf{C}}_V$, also $\{\hat{\kappa}_{V,n}, \hat{\mu}_{V,n}\}_{n=1}^N$ for each frequency, the noise variance estimate $\hat{\sigma}_V^2$. We set $\sigma_{n \rightarrow m}^2 = \hat{C}_{V,nn}$ and $x_{n \rightarrow m} = \hat{x}_{V,n}$, $\mu_{n \rightarrow m} = \hat{\mu}_{V,n}$, $\kappa_{k \rightarrow m} = \hat{\kappa}_{V,n}$, $\forall n$. The noise variance is initialized as $\hat{\sigma}_V^2$. The EPLSE is summarized as Algorithm 1.

The computation complexity of each steps of EPLSE algorithm is summarized as Table II. In general we set $M = N$, and the computation complexity is $O(M^3)$ in each iteration. In practice, the algorithm can be implemented efficiently with the MATLAB *bsxfun* function.

Implementation Details: To implement the EPLSE algorithm, the following strategies are proposed to enhance the robustness.

- The prior probability π_n is updated as λ_n (63a). Numerical results show that EPLSE may overestimate the model order and output two closely spaced frequencies with comparable magnitude. Numerically it is found that during the iteration, the prior probabilities of the two closely frequencies are almost one, and EPLSE does not combine the two frequencies as a single frequency. Thus, we restrict π_n to $[\pi_{\min}, 1 - \pi_{\min}]$, where $\pi_{\min} > 0$ is set as $\pi_{\min} = 5 \times 10^{-3}$.

Algorithm 1 EPLSE algorithm

-
- 1: Initialize $x_{k \rightarrow m}$ and $\sigma_{n \rightarrow m}^2$, $\mu_{n \rightarrow m}$, $\kappa_{k \rightarrow m}$, $\mathbf{z}_A^{\text{ext}}$, $\mathbf{v}_A^{\text{ext}}$. Set the number of outer iterations T_o and the threshold $\gamma = 0.5$ to determine the model order;
 - 2: **for** $t_{\text{outer}} = 1, \dots, T_{\text{outer}}$ **do**
 - 3: Update $m_{z \rightarrow \delta}(\mathbf{z})$ (Section III-A).
 - 4: **for** $t_{\text{inner}} = 1, \dots, T_{\text{inner}}$ **do**
 - 5: Compute $\tilde{m}_{m \rightarrow n}(\theta_n)$ (Section III-B).
 - 6: Update $m_{n \rightarrow m}(\theta_n)$ (Section III-C).
 - 7: Compute $\tilde{m}_{m \rightarrow n}(x_n)$ (Section III-D).
 - 8: Update $m_{n \rightarrow m}(x_n)$ (Section III-E).
 - 9: **end for**
 - 10: Compute $m_{\delta \rightarrow z}$ (Section III-F).
 - 11: **end for**
 - 12: Return $\hat{\theta}_n = \tilde{\mu}_n$ (38), $\hat{x}_k = \hat{m}_k$ (54), and $\hat{K} = \sum_{n=1}^N 1\{\pi_n^{\text{new}} > \gamma\}$.
-

TABLE II
COMPUTATION COMPLEXITY

Step	Complexity
Update $m_{z \rightarrow \delta}(\mathbf{z})$	$O(N)$
Compute $\tilde{m}_{m \rightarrow n}(\theta_n)$	$O(MN^2)$
Update $m_{n \rightarrow m}(\theta_n)$	$O(M^2N)$
Compute $\tilde{m}_{m \rightarrow n}(x_n)$	$O(MN^2)$
Update $m_{n \rightarrow m}(x_n)$	$O(M^2N)$
Compute $m_{\delta \rightarrow z}$	$O(N)$
All	$O(M^2N)$

- Update $\tilde{m}_{m \rightarrow n}(x_n)$ (50) involves dividing $\lambda_{n \rightarrow m}$. For small κ and $m > 1$, $|\lambda_{n \rightarrow m}|$ can be very small, which causes $|\tilde{x}_{m \rightarrow n}$ and $\tilde{\sigma}_{m \rightarrow n}^2$ to be very large. As a result, we restrict $\sigma_{m \rightarrow n}^2$ to $[\text{var}_{\min}, \infty]$, where $\text{var}_{\min} > 0$ is close to 0. Here we set $\text{var}_{\min} = 10^{-16}$. In this setting, EPLSE combines the two frequencies as a single frequency.
- Numerically we find that setting the number of inner iterations T_{inner} greater than 1 is beneficial for the robustness of EPLSE for nonlinear measurements scenario. For linear measurement scenario, we set $T_{\text{inner}} = 1$. For the nonlinear measurement scenario, the inner iteration is stopped when the

relative change of updated λ is small or the inner iterations exceeds $T_{\text{inner}} = 30$.

IV. NUMERICAL SIMULATION

In this section, the performance of EPLSE is evaluated by performing numerical simulations. In addition, EPLSE is compared with VALSE [23] under different scenarios.

Simulation Setup: The simulation is almost the same as [23]. For completeness, we present the details. The frequencies $\{\tilde{\theta}\}_{k=1}^K$ is drawn from $\mathcal{U}(-\pi, \pi)$ and the minimum wrap-around distance $\Delta\theta$ of the frequencies is $\Delta\theta = 2\pi/N$. The complex coefficients $\{\tilde{x}\}_{k=1}^K$ are generated by drawing their magnitudes from $\mathcal{N}(1, 0.2)$ and phases from $\mathcal{U}(-\pi, \pi)$. For the additive measurement noise model (4), The SNR is defined as $\text{SNR} = 10 \log \frac{\|\mathbf{z}\|_2^2}{\mathbb{E}\|\mathbf{w}\|_2^2} = 10 \log \frac{\|\mathbf{z}\|_2^2}{M\sigma_w^2}$, where σ_w^2 denotes the variance of the additive noise \mathbf{w} .

For both the EPLSE and VALSE algorithm, no prior information about the frequencies is assumed, and we set $p(\theta_n) = 1/(2\pi)$, $n = 1, \dots, N$. Both EPLSE and VALSE stop at iteration t if $\|\hat{\mathbf{z}}(t) - \hat{\mathbf{z}}(t-1)\|/\|\hat{\mathbf{z}}(t)\| < 10^{-6}$ or the number of iterations reaches 2000. For the assumed number of sinusoids N , we set $N = M$.

Three performance metrics are used:

- The normalized mean squared error of signal reconstruction: $20 \log \frac{\|\hat{\mathbf{z}} - \mathbf{z}\|_2}{\|\mathbf{z}\|_2}$,
- The empirical probability of successfully estimating the model order $\Pr(\hat{K} = K)$.
- The frequency estimation error $20 \log \|\hat{\boldsymbol{\theta}} - \boldsymbol{\theta}\|_2$ (dB) averaged over the trials in which the model order is estimated correctly.

At first, a simple simulation is conducted to show the recovery results of EPLSE. We set $M = 21$, $|\mathcal{M}| = 18$ which corresponds to the incomplete data case, $K = 3$, and the true frequencies and complex coefficients are $\boldsymbol{\theta} = [-2.1050, 1.4278, 2.4550]^T$ and $\mathbf{x} = [1.3154 + 0.1524j, 0.6064 - 0.2788j, 0.6544 - 0.5616j]^T$, respectively. The SNR is set as 10 dB. The results are shown in Fig. 8. It can be seen that EPLSE performs well and the model order is estimated correctly.

A. Performance versus SNR

The performance of EPLSE versus SNR is investigated. Parameters are set as follows: $M = 21$ and $K = 5$. Results are shown in Fig. 9. For the signal reconstruction and frequency estimation error, EPLSE achieves the same as that of VALSE except a small performance degradation at $\text{SNR} = 5$ dB. For $\text{SNR} \leq 15$ dB, the model order probability of VALSE is higher than that of EPLSE. As SNR increases, their model order probabilities are almost the same.

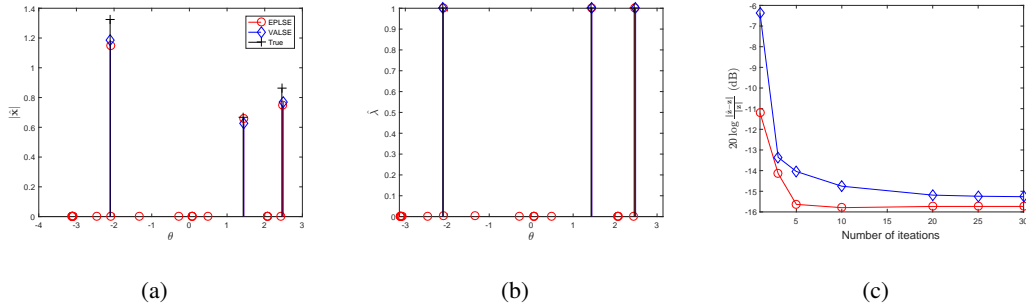


Fig. 8. A single realization of the performance of EPLSE. Fig. 8(a), Fig. 8(b) and Fig. 8(c) correspond to the amplitude reconstruction \hat{x} , the sparsity λ , signal reconstruction error, respectively.

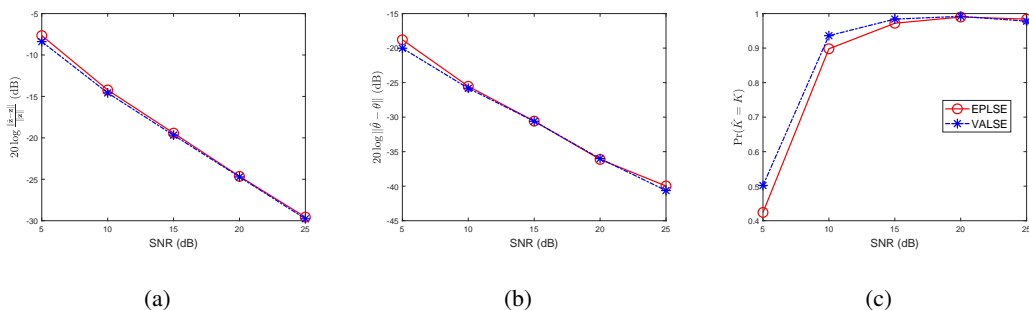


Fig. 9. Results versus SNR averaged over 500 MC trials. Fig. 9(a), Fig. 9(b) and Fig. 9(c) correspond to the signal reconstruction error, frequency estimation error and model order recovery probability, respectively.

B. Performance with Number of Measurements

The performance versus the number of measurements are investigated. The number of spectral is $K = 3$ and SNR = 20 dB. Results are shown in Fig. 10. It can be seen that the signal reconstruction and frequency estimation error of EPLSE is higher than that of VALSE. As for the model order probability, EPLSE is higher than VALSE.

C. Performance with Number of Spectra

We investigate the performance of EPLSE when the number of spectral K is varied. We set $M = 21$, SNR = 20 dB. It can be seen that EPLSE achieves almost the same performance as VALSE in terms of signal reconstruction and frequency estimation error. As for the model order estimation probability, EPLSE performs better.

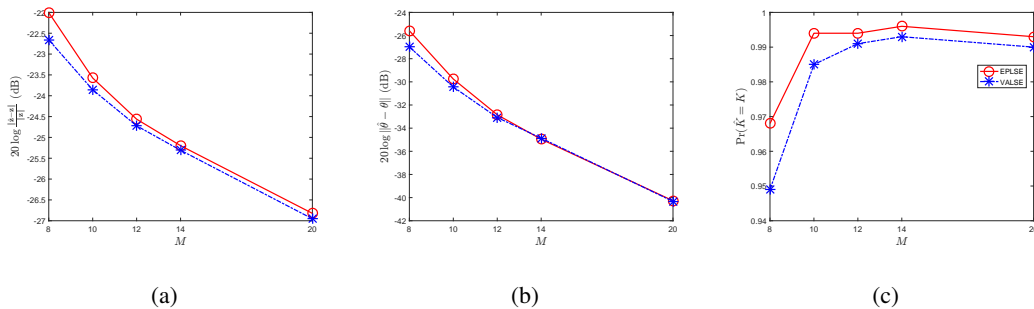


Fig. 10. Results versus M averaged over 1000 MC trials. Fig. 9(a), Fig. 9(b) and Fig. 9(c) correspond to the signal reconstruction error, frequency estimation error and model order recovery probability, respectively.

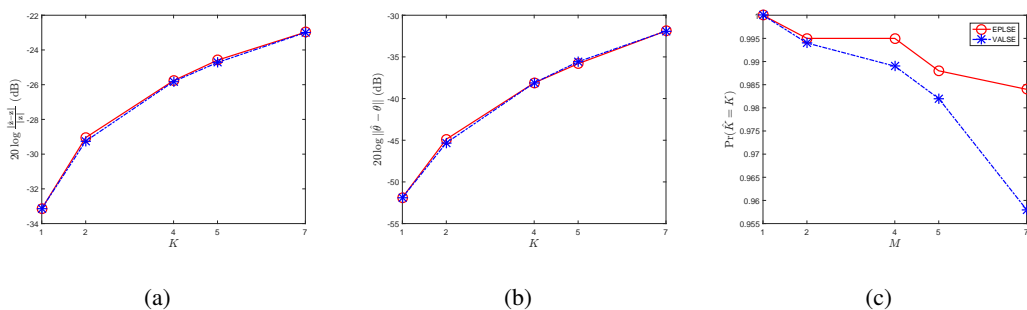


Fig. 11. Results versus K averaged over 1000 MC trials. Fig. 9(a), Fig. 9(b) and Fig. 9(c) correspond to the signal reconstruction error, frequency estimation error and model order recovery probability, respectively.

D. Estimation from Nonlinear (Quantized) Measurements

Here we illustrate the performance of Gr-EPLSE through low precision quantized measurements. We set $N = M = 41$ and $K = 3$. The results are shown in Fig. 12. For one-bit quantization, zero threshold is chosen and the amplitude information is lost in noiseless setting, thus the debiased NMSE (dNMSE) $\min_{c \in \mathbb{C}} 20 \frac{\|c\hat{\mathbf{z}} - \mathbf{z}\|_2}{\|\mathbf{z}\|_2}$ is used instead. For multi-bit quantization, a uniform quantizer is chosen. The real and imaginary parts of the measurements are quantized separately, and the dynamic range of the quantizer is restricted to be $[-3\sigma_z/\sqrt{2}, 3\sigma_z/\sqrt{2}]$, where σ_z^2 is the variance of \mathbf{z} . In our setting we have $\sigma_z^2 \approx K$. For 1 bit quantization, we input the noise variance to be 1 and for multi-bit quantization, (25) is used to iteratively estimate the noise variance.

Results are shown in Fig. 12. It can be seen that EPLSE converges, and the performance improves as bit depth or SNR increases.

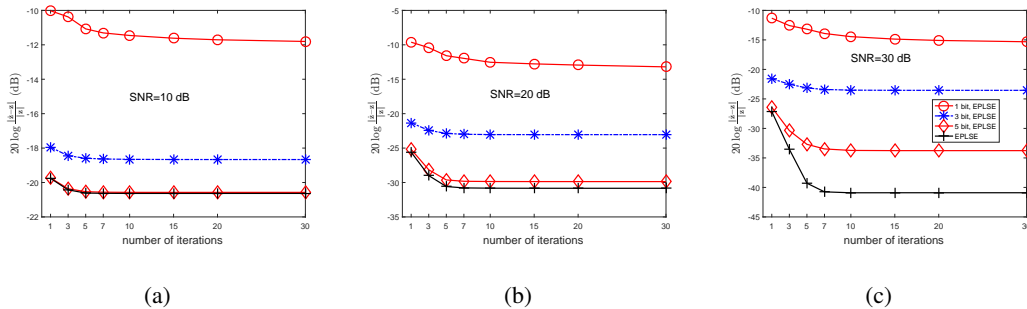


Fig. 12. The NMSE versus iteration averaged over 20 MC trials. Fig. 12(a), Fig. 12(b) and Fig. 12(c) correspond to the SNR 10 dB, 20 dB and 30 dB, respectively.

V. CONCLUSION

This paper proposes EPLSE algorithm for LSE. By incorporating the Bernoulli Gaussian distribution for sparsity and EM algorithm, EPLSE automatically estimates the model order, noise variance. In addition, EPLSE provides the posterior PDF of the frequencies, which is beneficial for sequential estimation. Numerical results demonstrate the excellent performance of EPLSE.

VI. APPENDIX

A. Motivation to use von Mises distribution

The motivation to use the VM distribution is three fold. First, VM distribution is the most commonly used distribution in circle, as Gaussian distribution in real line. The PDF of the VM distribution of a frequency is [35, p. 36]

$$p(\theta) = \mathcal{VM}(\theta; \mu, \kappa) = \frac{1}{2\pi I_0(\kappa)} e^{\kappa \cos(\theta - \mu)}, \quad (69)$$

where μ and κ are the mean direction and concentration parameters respectively, $I_p(\cdot)$ is the modified Bessel function of the first kind and the order p [35, p. 348]. Note that $\kappa = 0$ corresponds to the uninformative prior distribution $p(\theta) = 1/(2\pi)$ [23]. In addition, VM distribution can also be parameterized by $\eta = \kappa e^{j\mu}$:

$$\mathcal{VM}(\theta; \eta) = \frac{1}{2\pi I_0(|\eta|)} e^{\Re\{\eta^* e^{j\theta}\}}. \quad (70)$$

The characteristic function $\phi_m = \mathbb{E}[e^{jm\theta}]$ of the VM distribution $\mathcal{VM}(\theta, \mu, \kappa)$ has closed form, i.e.,

$$\phi_m = e^{jm\mu} \frac{I_m(\kappa)}{I_0(\kappa)}. \quad (71)$$

Note that $|\mathbb{E}[e^{jm\theta}]| < 1$ due to $I_{m-1}(\kappa) < I_0(\kappa)$, which is biased. However, this biased property is beneficial for estimation. For κ being large, the bias is small as $I_{m-1}(\kappa) < I_0(\kappa)$ approaches one, while

for κ being small, it is believed that the signal may not consists of this spectral, and the contribution of this line spectral for the observation is small as $I_{m-1}(\kappa)/I_0(\kappa)$ approaches zero.

Secondly, the VM distribution is closed under multiplication, i.e.,

$$\mathcal{VM}(\theta; \eta_1)\mathcal{VM}(\theta; \eta_2) \propto \mathcal{VM}(\theta; \eta), \quad (72)$$

where $\eta = \eta_1 + \eta_2$. That is, the product of two VM distribution is proportional to a VM PDF with mean direction $\angle(\eta_1 + \eta_2)$ and concentration $|\eta_1 + \eta_2|$. This result is useful for the derivation of EPLSE.

Finally, the VM distribution preserves the local structure of the PDF of the true posterior PDF. Let's take an example to show that. Assume a single sinusoid and

$$\mathbf{y} = \mathbf{a}(\theta)x + \mathbf{w}, \quad (73)$$

where $x \sim \mathcal{CN}(x; 0, \sigma_x^2)$. Let the prior distribution of θ be $p(\theta) = 1/(2\pi)$, then the posterior PDF of θ is

$$p(\theta|\mathbf{y}) = \frac{\int p(\mathbf{y}|\mathbf{x}, \theta)p(x)p(\theta)dx}{\int p(\mathbf{y}|\mathbf{x}, \theta)p(x)p(\theta)dx d\theta}. \quad (74)$$

For $\sigma_x^2 \rightarrow \infty$ (improper ‘‘flat’’ prior of x), we have [23]

$$p(\theta|\mathbf{y}) \propto e^{|\mathbf{y}^H \mathbf{a}(\theta)|^2 / (M\sigma^2)}. \quad (75)$$

Note that exponent of (75) is the periodogram scaled by $1/\sigma^2$. As shown in [23], the von Mises PDF approximation picks up the highest lobe. Here we show that the local structure is well preserved.

We approximate $p(\theta|\mathbf{y})$ as a von Mises distribution $\mathcal{VM}(\theta; \hat{\mu}, \hat{\kappa})$. For a non-VM PDF

$$p(\theta) = \frac{1}{C} e^{-g(\theta)}, \quad (76)$$

where C is a constant to ensure that PDF $p(\theta)$ is normalized. The approximation takes two steps: First, find $\hat{\mu}$ such that

$$\mu = \underset{\theta}{\operatorname{argmin}} g(\theta), \quad (77)$$

then obtain $\hat{\kappa}$ such that

$$\hat{\kappa} = A^{-1} \left(e^{-\frac{1}{2g(\hat{\mu})}} \right), \quad (78a)$$

where the detail of the inverse of $A(\cdot) \triangleq \frac{I_1(\cdot)}{I_0(\cdot)}$ is given in [35]. For (75), it can be decomposed as a mixture of the von Mises distribution, as shown in [23]. Then one picks the most dominant component and perform Newton refinement to obtain μ .

Here we take a simple example to show the effectiveness of the approximation. We set $N = 21$, $\theta = 1$, $g(\theta) = -|\mathbf{y}^H \mathbf{a}(\theta)|^2 / (M\sigma^2)$. We present a single realization of the true posterior PDF (75), and use the

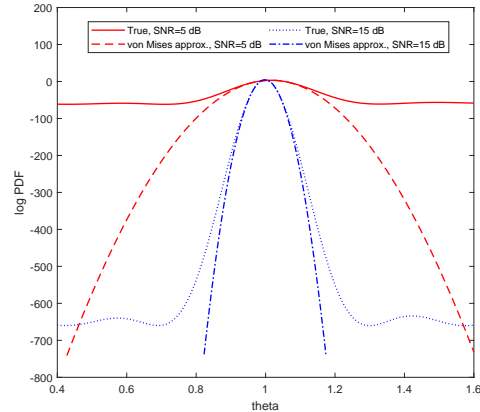


Fig. 13. The VM approximation of the true posterior PDF.

above two step to obtain the approximation of the VM distribution. The results are shown in Fig. 13. It can be seen that the local structure of the true posterior PDF around the peak are well preserved under low SNR (5 dB) and high SNR scenario (15 dB).

REFERENCES

- [1] P. Stoica and R. L. Moses, *Spectral Analysis of Signals*. Upper Saddle River, NJ, USA: Prentice-Hall, 2005.
- [2] W. Bajwa, A. Sayeed, and R. Nowak, “Compressed channel sensing: A new approach to estimating sparse multipath channels,” *Proc. IEEE*, vol. 98, pp. 1058-1076, Jun. 2010.
- [3] T. L. Hansen, P. B. Jørgensen, M. A. Badiu and B. H. Fleury, “An iterative receiver for OFDM with sparsity-based parametric channel estimation,” *IEEE Trans. Signal Process.*, vol. 66, no. 20, pp. 5454-5469, 2018.
- [4] P. Stoica and A. Nehorai, “Music, maximum likelihood and Cramér-Rao bound: further results and comparisons,” *IEEE Trans. Acoust., Speech, Signal Processing*, vol. 38, no. 12, pp. 2140-2150, Dec. 1990.
- [5] B. Ottersten, M. Viberg and T. Kailath, “Analysis of subspace fitting and ML techniques for parameter estimation from sensor array data,” *IEEE Trans. Signal Process.*, vol. 40, pp. 590-600, Mar. 1992.
- [6] R. Schmidt, “Multiple emitter location and signal parameter estimation,” *IEEE Trans. on Antennas and Propagation*, vol. 34, no. 3, pp. 276-280, 1986.
- [7] R. Roy and T. Kailath, “ESPRIT - estimation of signal parameters via rotational invariance

- techniques,” *IEEE Trans. on Acoustics, Speech and Signal Processing*, vol. 37, no. 7, pp. 984-995, 1989.
- [8] D. Malioutov, M. Cetin and A. Willsky, “A sparse signal reconstruction perspective for source localization with sensor arrays,” *IEEE Trans. Signal Process.*, vol. 53, no. 8, pp. 3010-2022, 2005.
- [9] Y. Chi, L. L. Scharf, A. Pezeshki, and R. Calderbank, “Sensitivity to basis mismatch in compressed sensing,” *IEEE Trans. Signal Process.*, vol. 59, no. 5, pp. 2182-2195, 2011.
- [10] L. Hu, Z. Shi, J. Zhou and Q. Fu, “Compressed sensing of complex sinusoids: An approach based on dictionary refinement” *IEEE Trans. Signal Process.*, vol. 60, no. 7, pp. 3809-3822, 2012.
- [11] L. Hu, J. Zhou, Z. Shi, Q. Fu, “A fast and accurate reconstruction algorithm for compressed sensing of complex sinusoids,” *IEEE Trans. Signal Process.*, vol. 61, no. 22, pp. 5744-5754, 2013.
- [12] B. Mamandipoor, D. Ramasamy and U. Madhow, “Newtonized orthogonal matching pursuit: Frequency estimation over the continuum,” *IEEE Trans. Signal Process.*, vol. 64, no. 19, pp. 5066-5081, 2016.
- [13] J. Zhu, L. Han, R. S. Blum and Z. Xu, “Multi-snapshot Newtonized orthogonal matching pursuit for line spectrum estimation with multiple measurement vectors,” *Signal Processing*, vol. 165, pp. 175-185, 2018.
- [14] J. Fang, F. Wang, Y. Shen, H. Li and R. S. Blum, “Superresolution compressed sensing for line spectral estimation: an iterative reweighted approach,” *IEEE Trans. Signal Process.*, vol. 64, no. 18, pp. 4649-4662, 2016.
- [15] V. Chandrasekaran, B. Recht, P. A. Parrilo, and A. S. Willsky, “The convex geometry of linear inverse problems,” *Foundations of Computational Mathematics*, vol. 12, no. 6, pp. 805-849, 2012.
- [16] Z. Yang, L. Xie and C. Zhang, “A discretization-free sparse and parametric approach for linear array signal processing,” *IEEE Trans. Signal Process.*, vol. 62, no. 19, pp. 4959-4973, 2014.
- [17] Z. Yang and L. Xie, “On gridless sparse methods for line spectral estimation from complete and incomplete data,” *IEEE Trans. Signal Process.*, vol. 63, no. 12, pp. 3139-3153, 2015.
- [18] Z. Yang and L. Xie, “Exact joint sparse frequency recovery via optimization methods,” *IEEE Trans. on Signal Process.*, vol. 64, no. 19, pp. 5145-5157, 2016.
- [19] Z. Yang, J. Li, P. Stoica, and L. Xie, “Sparse methods for direction-of-arrival estimation,” *Academic Press Library in Signal Processing*, vol. 7, pp. 509-581. Academic Press, 2018.
- [20] Y. Li and Y. Chi, “Off-the-grid line spectrum denoising and estimation with multiple measurement vectors,” *IEEE Trans. Signal Process.*, vol. 64, no. 5, pp. 1257-1269, 2016.
- [21] Y. Chen and Y. Chi, “Robust spectral compressed sensing via structured matrix completion,” *IEEE Trans. Inf. Theory*, vol. 60, no. 10, pp. 6576-6601, Oct. 2014.

- [22] Z. Yang and L. Xie, “Enhancing sparsity and resolution via reweighted atomic norm minimization,” *IEEE Trans. Signal Process.*, vol. 64, no. 4, pp. 995-1006, Feb. 2016.
- [23] M. A. Badiu, T. L. Hansen and B. H. Fleury, “Variational Bayesian inference of line spectral,” *IEEE Trans. Signal Process.*, vol. 65, no. 9, pp. 2247-2261, 2017.
- [24] J. Zhu, Q. Zhang, P. Gerstoft, M. A. Badiu and Z. Xu, “Grid-less variational Bayesian line spectral estimation with multiple measurement vectors,” *Signal Processing*, vol. 61, pp. 155-164, 2019.
- [25] D. L. Donoho, A. Maleki, and A. Montanari, “Message passing algorithms for compressed sensing: I. Motivation and construction” in *Proc. Inf. Theory Workshop*, Cairo, Egypt, Jan. 2010, pp. 1-5.
- [26] S. Rangan, “Generalized approximate message passing for estimation with random linear mixing,” in *Proc. IEEE Int. Symp. Inf. Theory*, Jul. 2011, pp. 2168-2172.
- [27] X. Meng, S. Wu, L. Kuang, and J. Lu, “An expectation propagation perspective on approximate message passing,” *IEEE Signal Process. Lett.*, vol. 22, no. 8, pp. 1194-1197, Aug. 2015.
- [28] S. Wu, L. Kuang, Z. Ni, J. Lu, D. Huang, and Q. Guo, “Low-complexity iterative detection for large-scale multiuser MIMO-OFDM systems using approximate message passing,” *IEEE J. Sel. Topics Signal Process.*, vol. 8, no. 5, pp. 902-915, May 2014.
- [29] Q. Zou, H. Zhang, C.-K. Wen, S. Jin, and R. Yu, “Concise derivation for generalized approximate message passing using expectation propagation,” *IEEE Signal Process. Lett.*, vol. 25, no. 12, pp. 1835-1839, Dec. 2018.
- [30] X. Meng, S. Wu and J. Zhu, “A unified Bayesian inference framework for generalized linear models,” *IEEE Signal Process. Lett.*, vol. 25, no. 3, pp. 398-402, 2018.
- [31] J. Zhu, “A comment on the “A unified Bayesian inference framework for generalized linear models,”” arXiv preprint, 2019.
- [32] T. Minka, “A family of algorithms for approximate Bayesian inference,” Ph.D. dissertation, Department of Electrical Engineering and Computer Science, Mass. Inst. Technol., Cambridge, MA, USA, 2001.
- [33] J. P. Vila and P. Schniter, “Expectation-maximization Gaussian-mixture approximate message passing,” *IEEE Trans. Signal Process.*, vol. 61, no. 19, pp. 4658-4672, Oct. 2013.
- [34] D. Zachariah, P. Wirfält, M. Jansson and S. Chatterjee, “Line spectrum estimation with probabilistic priors,” *Signal Processing*, vol. 93, no. 11, pp. 2969-2974, 2013.
- [35] K. V. Mardia and P. E. Jupp, *Directional Statistics*. New York, NY, USA: Wiley, 2000.
- [36] U. S. Kamilov, V. K. Goyal, and S. Rangan, “Message passing de-quantization with applications to compressed sensing,” *IEEE Trans. Signal Process.*, vol. 60, no. 12, pp. 6270-6281, 2012.
- [37] P. Schniter and S. Rangan, “Compressive phase retrieval via generalized approximate message

- passing,” *IEEE Trans. Signal Process.*, vol. 63, no. 4, pp. 1043-1055 Feb. 2015.
- [38] J. Zhu, Q. Yuan, C. Song and Z. Xu, “Phase retrieval from quantized measurements via approximate message passing,” *IEEE Signal Process. Lett.*, vol. 26, no. 7, pp. 986-990, 2019.
- [39] S. Wang, L. Zhang and Y. Li, “Multiuser MIMO transmission aided by massive one-bit magnitude measurements,” *IEEE Trans. Wireless Commun.*, vol. 15, no. 10, pp. 7058-7073, Oct. 2016.
- [40] Z. He, H. Li, Z. Shi, J. Fang and L. Huang, “A robust iteratively reweighted L_2 approach for spectral compressed sensing in impulsive noise,” *IEEE Signal Process. Lett.*, vol. 24, no. 7, pp. 938-942, 2017.
- [41] X. Meng and J. Zhu, “Bilinear adaptive generalized vector approximate message passing,” *IEEE Access*, vo. 7, pp. 4807-4815, 2018.